HHU/iw

MPS/SM/Note 74-15
Revised 31.10.1974.

THE MEASUREMENT, PRESENTATION AND INTERPRETATION OF COUPLING IMPEDANCE DATA

H.H. Umstätter

CONTENTS

1. Abstract

After a simple explanation of the word "coupling impedance", the problems encountered in any attempt to measure distributed impedances beyond 20 MHz by straight forward low frequency measurements are discussed. The large vacuum tanks which are mostly filled with complicated equipment behave like the distributed circuits encountered in microwave equipment and therefore the measurement of reflection coefficients is more adequate. Therefore, guided by a typical example, the recent measurements on septum magnet s.s. 74, the close relations between the reflection coefficient in the frequency domain and the impedance plots in a Smith chart and Carter Chart and its role as element of the scattering matrix are reviewed for our application in hopefully clear terms for those who will measure in the future and accelerator theorists who are interested in the interpretation of the data. It is then compared with the reflection coefficient in the time domain via the Laplace transform and it is found that time domain reflectometer measurements give most and the most easily interpretable information about coupling impedances. For the tank of the septum magnet S.S. 74 one finds $Z/n = 1.3\ \Omega$ at 69 MHz.

2. What is the Coupling Impedance?

There is no simple answer and an enormous number of theoretical reports have been written on many differentmmechanisms which could cause instabilities. We certainly don't mean a piece of hardware (although drawings with the title "coupling impedance" existed). So an answer to non-specialists should be given: In simple cases the coupling impedance is the measurable impedance value Z_c of a vacuum chamber wall. Examples are the impedance across the gap of an accelerating RF cavity or the capacitive impedance of a vacuum flange or the 0.1Ω resistance of our short ceramic vacuum chambers with resistive metal coating. In these cases the beam current i_b (= charge/revolution period) induces an equal return current i_b in the wall and as this wall current is forced to flow through the sum Z_c of all wall impedances, it induces a voltage which disturbs the beam:

$$V_b = i_b \cdot Z_c \tag{1}$$

The coupling impedance concept is, however, more general. Even if the walls of a large vacuum tank are perfectly conducting, there is a coupling impedance because the walls reflect the electromagnetic wave which goes out from the bunches (as in a cavity resonator) and the reflected longitudinal electric field E perturbs the particles. The integral over this E-field along the particle orbit is the beam induced voltage V_b per turn. This voltage V_b divided by the beam current i_b is the longitudinal coupling impedance

$$Z_c = \frac{\int E d\ell}{i_b} = \frac{V_b}{i_b} \tag{2}$$

Such coupling impedance contributions which involve an integral cannot be measured by attaching an RF bridge to two terminals, but are nevertheless important (e.g. for negative mass instability). One can derive them from time domain reflectometer measurements. Time domain reflectometer measurements allow to directly determine resistive wall effects and relative changes of beam potential resulting from changes of chamber cross-sections (in the same way as characteristic impedance of cables).

This is necessary in all the analytically untreatable geometries encountered in practice (e.g. beam potential in front of a septum magnet placed in an excentric rectangular tank). The beam induces also transverse fields $E_\perp$ and there exists also a transverse coupling impedance $Z_\perp = \int E_\perp dl/i_b$. Obviously stable particle acceleration requires that the induced voltage $Z_c \cdot i_b$ must remain small compared with the voltage of the accelerating RF-cavities. It must be far smaller when the cavities are switched off (debunching for continuous transfer), because then the beam becomes the victim of these voltages only and its small momentum spread is blown up. Therefore, if we want higher beam current i_b, we must measure and reduce the coupling impedance Z_c everywhere in the PS. The coasting beam criterion specifies limits on Z_c for the PS[1,2,3].

3. The scope and limitations of routine measurements.

When the equipment is measured it must be completely assembled as it will be later in the PS and, there is therefore not much time to spend on impedance measurements. The measurements are usually done by one person on part time and without transport to an electronic lab but on the vacuum test stand or in an assembly hall or in a PS shut down under adverse conditions in the ring. Yet one can record as much as possible about the complex impedances and do this for all kinds of equipment in straight sections by the same common method [9-11]. It must be possible to compare such different things as an RF-cavity with a septum magnet or LINAC inflector tank impartially and find out later when the equipment is inaccessibly installed which is the most likely candidate to have caused some actually observed self-bunching phenomenon or instability. At this stage, modifications are already costly (Therefore it is better to provide them already at the design stage by a discussion with the author as in the case of FAK). The measurements should cover a continuous spectrum from 150 kHz to 1000-2000 MHz, if possible, so that no resonance peak is overlooked. We shall first discuss impedance measurements in the frequency domain because people are more familiar with it and after encountering the difficulties discuss them in the time domain where measurements are more easily interpretable over wide bandwidth.

4. Direct impedance measurements in the frequency domain.

4.1 If the wall impedance is concentrated on a short gap in the vacuum chamber (e.g. accelerating gap or vacuum flange) it can be measured directly up to 100 MHz or more with an RF bridge but this is not possible with distributed impedances :

4.2 The hp-vector impedance meter is connected to one open end (upstream) of the vacuum tank. In order to connect the meter with the downstream end of the tank a straight conductor of 1 cm diameter is placed in beam position in the vacuum tank with a 125 Ω series resistor at the far end. The wall impedance seen from the inside is measured in magnitude and phase (Table 1) on septum tank SS 74 (June 1974) over the frequency range 500 kHz to 100 MHz and plotted in Fig.1.
Corrections : One can split this complex input impedance Z into its resistance and reactance

$$Z = |Z|\, e^{i\phi} = R + jX \qquad (3)$$

and subtract again the 125 Ω from its real part to obtain the wall impedance or coupling impedance at low frequency

$$Z_c = (R - 125\ \Omega) + jX$$

The reason for this addition and subtraction of 125Ω is the following : The 1 cm conductor, in spite of its big diameter, has a non negligible lead inductance. If the end would be connected to the wall (short to ground) this lead inductance which is not exactly known because it depends on the inner tank geometry would add an important series reactance $jX = j\omega L$, and increase Z. If one leaves the end open or inserts a high resistor, the parasitic capacity of the conductor to the wall shunts Z and diminishes it. These two effects balance over a wider range of frequency (up to quadratic terms) if the small wall resistance is increased by a series resistor of

$$Z_o = \sqrt{L/C}$$

Our conductor meets this condition at least for the standard PS-vacuum chamber. Thus the addition and subtraction of 125 Ω extends the validity of such direct measurements up to about 10 MHz.
Then the quarter wavelength ($\lambda/4$ = 7.5 m) becomes comparable to the tank length as in microwave circuits and one has to account for impedance transformations on transmission lines and adopt methods and definitions like the reflection coefficient which proved to be more useful in this field

5. Simulating the geometry in the test set-up.

Our vacuum tanks are finally inserted between the long standard elliptic (70 mm x 146 mm) PS-vacuum chambers in the bending magnets. Therefore for simulation one could attach such chambers to both ends of the tank under test and extend the centre conductor. Then these long chambers form coaxial transmission lines of well-defined characteristic impedance*)

$$Z_o = 60\ \Omega\ \ell n\ \frac{4.318\ \text{cm}}{a} \qquad (a = \text{conductor radius}) \quad (4)$$

and can be matched at the down-stream end by a resistor and at the up-stream end by the generator's source impedance Z_o. The source impedance must be high for two reasons :

1) The common standard Z_o = 50 Ω would require a very thick centre conductor of 3.8 cm diameter which is not typical for a beam diameter.

*) This formula is valid for a << 4.318 cm (= equivalent radius of PS vacuum chamber) and has been derived analytically from a conformal mapping of the TEM field, See Fig. 1 of Ref. 4.

2) The more important reason is that the beam behaves like a current generator which can excite very high voltages $Z_c \cdot i_b$ (for instance in resonant cavities) and such a generator should be simulated by increasing the source resistance ($Z_o \to \infty$). However if one tries to match the PS-vacuum chamber to a high source resistance this requires an extremely thin centre conductor (e.g. $5 \cdot 10^{-6}$ mm diameter for 1 kΩ) which is not feasible in practice because much of the signal power does not follow the wire but propagates in a damped waveguide mode and perturbs measurements. Nevertheless an increased Z_o is preferable also because equal relative changes of vacuum chamber diameters correspond to the same absolute but smaller relative changes in characteristic impedance and thus the transmitted test signal is less affected by mismatches whereas the reflected signal can still be measured.

Therefore, all our measurements are referred to $Z_o = 125\ \Omega$, the highest standard impedance for which precise coaxial connectors and cables are available. A centre conductor of a = 0,5 cm matches Z_o approximately to the standard PS-vacuum chamber as reference level. (Sometimes measurements are repeated with a = 1 mm). The (skin effect) resistance of the 0.5 cm conductor is neglected because it is $\ll \frac{1\Omega}{m}$.
Now the infinitely long or perfectly matched line can be replaced by short matched pieces of vacuum chamber (e.g. bellows) and these terminations on both ends are represented in the equivalent circuit by the source and load resistors of $Z_o = 125\ \Omega$:

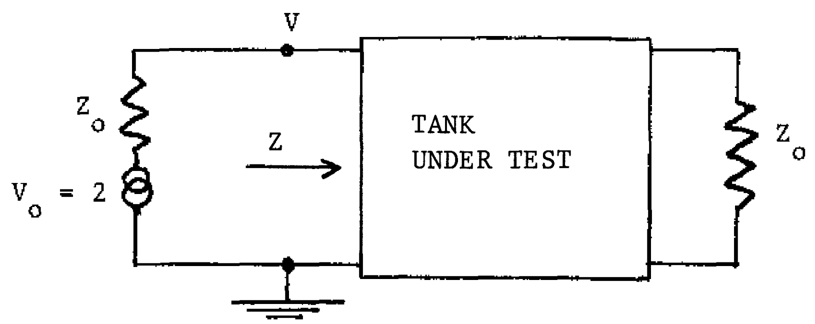

6. S-paramèters and the scattering matrix

This test set up evolved from two considerations :

1) Minimize the effects of parasitic capacities and lead inductances to extend the validity of direct, uncorrected RF-measurements to a wider frequency range.

2) Simulate the geometrical configuration of a non-standard tank in a PS straight section inserted between two long standard PS vacuum chambers in which a sinusoidal signal or a moving charge (= current pulse) propagates with relativistic velocity in beam position on the surface of a guiding conductor of approximate beam diameter and which, in addition to its normal behaviour, excites voltages which, in the case of the actual accelerator, act back on the beam and which, in our case, also affect the transmitted test pulse. However more important is that in our case these excited voltages of scattered waves are guided by the centre conductor and propagate forward and backward (in a well-defined TEM-mode) to an instrument where they can be measured. By raising the characteristic impedance Z_o one can reduce the reflected power (just measurable) with the result that the transmitted test signal is very little affected. (This is a special case of the general principle that a measuring instrument should draw only a small fraction of power from the measured object).

This test set up with equal source and load impedances Z_o is actually a test set up for measuring "S-parameters", the 4 complex elements of the scattering matrix or "S-matrix", which completely describes a linear network with only two accessible terminals (a "two-port" or "4-pole network", considered as a "black box" to be explored) :

$$\begin{aligned} b_1 &= s_{11}\, a_1 + s_{12}\, a_2 \\ b_2 &= s_{21}\, a_1 + s_{22}\, a_2 \end{aligned} \qquad (5)$$

$$S(\omega) = \begin{bmatrix} s_{11} & s_{12} \\ s_{21} & s_{22} \end{bmatrix} \qquad (6)$$

Without going into details about the significance of scattering variables a, b[5)7)], let us just mention that our measured input impedance Z is directly related to s_{11} and that the diagonal elements s_{11}, s_{22}, the (voltage) reflection coefficients, were also denoted as ρ_1, ρ_2 or Γ_1, Γ_2 long before the whole scattering matrix came into use. The off-diagonal elements s_{12}, s_{21} are the reverse and forward transmission coefficients. These four S-parameters form a consistent set of data without redundancy from which all input/output impedances and transfer impedances in other words all elements of the impedance matrix (z-parameters) or admittance matrix (y-parameters) can be computed[*)]. This becomes necessary at higher frequencies as measurements of impedances become inaccurate or impossible[6)].

The (generalized) S-parameters are defined in such a way[5)] that their magnitudes represent square roots of power ratios of reflected to incident or transmitted to incident powers in each of the two directions. As a consequence in a **lossless** (purely reactive) network the transmitted power is the difference between incident and reflected power.

$$|s_{12}|^2 = 1-|s_{11}|^2 \quad \text{and} \quad |s_{21}|^2 = 1-|s_{22}|^2$$

Since powers and voltages of travelling waves on lossless transmission lines (attached PS-vacuum chambers) don't change their magnitude, the magnitude of s-parameters is also constant and only their phases rotate linearly along the lines. This opens the way to more correct data in the range 10-100 MHz where the distance between instrument and center of a tank under test amounts to many short wavelengths. Above 1 GHz a new limit is encountered : Transformation of our guided TEM-mode into TM and TE-waveguide modes which propagate more easily, exhibit dispersion and disturb the measurements.

---

*) A whole "Microware program library" is supplied by HEWLETT-PACKARD for the programmable desk calculators 9820 which allows to handle S-parameters.

7. The reflection coefficient in the frequency domain $\rho(\omega)$

The generator voltage in the equivalent circuit is chosen to be $V_o = 2$ and its source impedance Z_o with the input impedance Z in series forms a voltage divider. Thus the input voltage will be

$$V = 2 \frac{Z}{Z + Z_o} \tag{7}$$

On the other hand the incident voltage on an infinitely long transmission line ($Z = Z_o$) would be = 1. The excess voltage V-1 is reflected. The ratio of reflected to incident voltage is the reflection coefficient ρ or Γ*).

$$\rho = \frac{V - 1}{1} = \frac{Z - Z_o}{Z + Z_o} \tag{8}$$

$$\rho = \frac{Z/Z_o - 1}{Z/Z_o + 1} = \frac{1 - Y/Y_o}{1 + Y/Y_o} \tag{9}$$

Here $Y_o = 1/Z_o$ and $Y = G + jB = (R - jX)/(R^2 + X^2) = 1/Z$ designate admittances. An instrument which measures the reflection coefficient (reflectometer) can be used to obtain the input impedance:

$$Z = Z_o \frac{\rho + 1}{\rho - 1} \tag{10}$$

ρ is actually the input reflection coefficient $\rho_1 = s_{11}$ on the upstream end of a straight section. The tank can be turned around to measure the output reflection coefficient $\rho_2 = s_{22}$ in the same way. This is not necessary if the tank and thus its scattering matrix are symmetric ($\rho_1 = \rho_2 = s_{11} = s_{22}$ $s_{12} = s_{21}$). A small FORTRAN program "CONVERT" was written which reads data from punched cards (Table 1) and returns another set of punched cards with

*) Attention, some classical books on reactance filter synthesis define ρ or Γ with opposite sign.

the reflection coefficient at the same frequencies for later use on computers (Table 2). This reflection coefficient is plotted in polar coordinates in Fig. 2 for septum magnet S.S. 74

Since the power and voltage of (forward and backward) travelling waves in lossless transmission lines is constant, the magnitude of ρ's and all other S-parameters does not depend on the length of line which may lie between the terminals of the measuring instrument and the obstacle. The waves on the two matched input and output transmission lines are only delayed by constant delays. For instance a small input transmission line (standard PS vacuum chamber) of length ℓ and delay $\tau = \ell/c$, (c=.2998 m/nsec) will delay the reflected wave by 2τ and thus shift the phase of the reflection coefficient by

$$\rho = -\omega 2\tau = -360^{\circ}.f.2\tau \tag{11}$$

Thus the transformed reflection coefficient becomes

$$\rho' = \rho . e^{-j\omega 2\tau} = \rho e^{\frac{-j\omega 2\ell}{c}} \tag{12}$$

This property of ρ allows to measure reflection coefficients remotedly and to make the necessary corrections by rotating back (clockwise) the reflection coefficient data in the polar diagram Fig. 2. The rotated reflection coefficient is substituted to obtain the true impedances $Z(\omega)$ in the shifted reflection coefficient plane.
(Similar corrections of 1τ and $\rho = -\omega\tau$ can be applied to the transmission coefficients).

8. Impedance plots in Carter and Smith charts

The reflection coefficient has the advantage that it maps the infinite resistance scale $0 \leqslant R \leqslant \infty$ on a finite $-1 \leqslant \rho \leqslant +1$ interval and for all complex impedances $R \geqslant 0$ and $-j\infty \leqslant jX \leqslant j\infty$ its magnitude is limited to $|\rho| \leqslant 1$ which fits into the circular screen of an oscilloscope whereas Z doesn't. Therefore network analysers often display the reflection coefficient with superimposed ohm-scales and impedance coordinates according to equations (8) or (9).*) Such an overlay with rectangular coordinates of resistance and reactance of Z is the Smith chart (Fig. 3). Another overlay with polar coordinates of magnitude and phase of Z is known as the Carter chart (Fig. 4). Thus the Smith chart and Carter chart are conformal maps of rectangular and polar coordinates into the reflection coefficient plane by means of the analytic function equ.(9). Both charts were called "transmission line calculators" in the original papers of P.S. CARTER and Ph. H. SMITH (35 years ago) because, when rotated over a polar coordinate plot of ρ according to equ.(12), they facilitate calculation of impedance transformations on transmission lines and waveguides and other manipulations of complex numbers. For instance the reciprocal of complex $Z/125\ \Omega$ is obtained by merely changing the sign of ρ or rotation of the charts by 180°. Addition and subtraction of complex Z is facilitated by transition from polar to rectangular coordinates i.e. from Carter to Smith chart, Fig.4→3. One could have plotted the impedance metre readings in Table 1 directly into the Carter chart (Fig.4) and copied on Fig.2 to obtain $\rho(\omega)$ without a computer. The Smith chart Fig.3 facilitates subtraction of the 125 Ω terminal resistance $R/Z_o = 1$ and makes it obvious that, at low frequencies (<5 MHz), only the reactance of Z increases at the rate of $jX(\omega)/\omega = 0{,}4$ µH It is a wall inductance ΔL due to the increased flux in the enlarged vacuum tank which is linked with the current in the centre conductor. However, for higher frequencies a single inductance doesn't explain $Z(\omega)$: One observes in the Carter chart that up to about 50 MHz the curve circulates slowly around a centre $Z/Z_o \simeq 1.44$ or 180 Ω. Therefore one

*) This doesn't mean that we have them in the PS.

could renormalize all data to $Z'_o = 180\ \Omega$ and plot them in another Carter chart and polar diagram of ρ where they are better centred and $|\rho|$ remains constant at least up to 50 MHz but rotates at the rate $\rho/f = -3^o/\text{MHz}$. According to equation (11) this means that a reflection is encountered after

$$\tau = \frac{\rho/f}{720^o} = 4.17 \text{ nsec}$$

or after an electrical length of $\ell = \tau . c = 1.2$ m, the approximate tank length. If all data $\rho(\omega)$ are rotated back, one obtains a constant $\rho \approx -0.2$ up to about 50 MHz and from 80 to 100 MHz but at around 66 MHz there remains a frequency dependence which, copied on a Smith chart, could be explained by the presence of a narrow-band resonant circuit. This example illustrates that even in the simplest and most frequently encountered cases the interpretation of wide band impedance measurements requires laborious transformations in the frequency domain.

The interpretation would be almost impossible if there were many more than one reflection which let $\rho(\omega)$ be the sum of several vectors rotating at various speeds! We shall see that one way to solve this problem is to treat the data on a computer and carry out the integral transform

$$f(\tau) = 2\int_0^\infty \rho(\omega) e^{+j\omega\tau} d\omega$$

which rotates back the complex reflection coefficients and integrates over all spectral contributions $0 \leqslant \omega < \infty$ which belong to the same delay τ. Then $f(\tau)$ allows to recognize all reflections which belong to the same τ. This is a Fourier transform or (with $j\omega = s$) a special case of the inverse Laplace transform, which transforms the data into the time domain. It can be saved if one observes the reflection coefficient $\rho(t)$ directly with a time domain reflectometer.

9. The reflection coefficient in the time domain $\rho(t)$

The test set for time domain reflectometry (TDR) consists essentially of a fast sampling oscilloscope for observation of incident, reflected and transmitted voltage and a step (pulse) generator of 125 Ω source impedance which replaces the continuous wave generator in our equivalent circuit. Equations (7) - (10) remain valid at least for resistive loads $Z = R$: The step generator rapidly switches on a constant voltage $V_o = 2$. The incident voltage which propagates along the input transmission line of $Z_o = 125\ \Omega$ is = 1 until it encounters the input resistance R and becomes

$$V = \frac{R}{R + 125\ \Omega} \tag{7a}$$

$V - 1$ is reflected and appears after the travel-around-time 2τ on the oscilloscope as a small step superposed on the incident step $V = 1$ or $\rho = 0$. The ratio of reflected to incident voltage is the reflection coefficient

$$\rho = \frac{V - 1}{1} = \frac{R - 125\ \Omega}{R + 125\ \Omega} \tag{8a}$$

In the general case when Z is complex, the voltage $V(t)$ is a transient function of t and $\rho(t)$ is still the ratio of reflected voltage to constant incident voltage at any instant $t > 0$. For dissipative loads ($Z = R + jX$ with $R > 0$) the transient $\rho(t)$ decays or reaches a constant level corresponding to the dc-resistance $Z(\omega) = R$ for $\omega \to 0$.
The inverse relation

$$R = 125\ \Omega\left(\frac{\rho + 1}{\rho - 1}\right) \tag{10a}$$

allows to place a vertical overlay scale with ohm-values on the display and read resistance values directly. (The real axis of a Carter or Smith chart overlay for $\rho(\omega)$ could be used).

10. Comparison of the reflection coefficients $\rho(\omega)$ and $\rho(t)$

The use of the letter ρ with different meanings for the reflection coefficient $\rho(t)$ in time domain and $\rho(\omega)$ in frequency domain is analogous to the letter V for voltage with two distinct meanings $V(t)$ or $V(\omega)$: When referring to the observed voltage on a charging condenser, one means $V(t)$ as a function of time, whereas when referring to the voltage drop on the reactance of a condenser one means

$$V(\omega) = Z(\omega) \cdot i(\omega) = \frac{1}{j\omega C} \cdot i(\omega) \tag{14}$$

and it is implied that $V(\omega)$ is the complex amplitude of a sinusoidal voltage characterized by amplitude and phase which are both functions of the frequency $s = j\omega = j2\pi f$. The same is true for the current $i(\omega)$ and this allows to define $Z(\omega)$ and $\rho(\omega)$ by division, multiplication, addition and subtraction.

More generally an arbitrary voltage pulse $V(t)$ can be decomposed into a continuous spectrum of complex amplitudes $V(j\omega)$ by evaluating the Laplace transform

$$V(s) = \int_0^{\infty} V(t)\ e^{-st}\ dt = L(V(t)) \tag{15}$$

thus $V(\omega)$ is the transform of $V(t)$*). The transition from the spectrum $V(j\omega)$ back into the time domain is accomplished by the inverse Laplace transform

$$V(t) = L^{-1}(V_{(s)}) \tag{16}$$

The direct Laplace transform can often be calculated analytically whereas the inverse Laplace transform requires a contour integral in the complex frequency plane and is more difficult to find. Therefore a computer program "RESPONS" has been written and used since several years by the

*) We should use $v(t)$, $i(t)$, $\rho(t)$ in the time domain and capital letters $V(\omega)$ $I(\omega)$ and $P(\omega)$ for their transforms but our choice is no more free. We distinguish them by the argument.

author to evaluate the inverse Laplace transform of measured data (like Table 1 or 2) or the product of measured and computed transforms and plot the resulting transient responses. Addition and subtraction of functions correspond to additions or subtractions of their transforms. Thus the inverse Laplace transform of the reflected spectrum

$$\rho(\omega) = V(\omega) - 1 \tag{17}$$

is

$$L^{-1}(\rho(\omega)) = V(t) - L^{-1}(1) = V(t) - \delta(t) \tag{18}$$

$\delta(t)$ is the unit impulse or Dirac function used as incident test pulse and $V-\delta$ the reflected voltage which results from it. Although such a test pulse of very short length high peak and unit integral $\int\delta(t)dt = 1$ would better simulate a short bunch of unit charge, it is less pratical for definition of the ratio of reflected to incident pulse. The unit step pulse or Heaviside function

$$h(t) = \begin{cases} = 0 \text{ for } t < 0 \\ = \frac{1}{2} \text{ for } t = 0 \\ = 1 \text{ for } t > 0 \end{cases} \tag{19}$$

is more pratical because the height of the incident pulse is constant = 1 and it also has a well-defined continuous spectrum

$$H(\omega) = \frac{1}{s} = \frac{1}{j\omega} \tag{20}$$

Multiplication of this incident pulse spectrum by $\rho(\omega)$ yields the reflected pulse spectrum. Its inverse Laplace transform is the reflection coefficient $\rho(t)$ in the time domain.

$$\rho(t) = L^{-1}\ (\rho(\omega) \cdot \frac{1}{j\omega t}) \tag{21}$$

The punched cards of reflection coefficient data (Table 2) have been read by the FORTRAN program RESPONS, multiplied by $1/j\omega$. The result is plotted in Fig. 5 for comparison with the photographed TDR signal in Fig. 6. One can see that the TDR-measurements contain far more details than the plot. This is because our measurements of $Z(\omega)$ are limited to 100 MHz bandwidth (and extrapolated in Fig. 2 to $\rho = 0$ at 150 MHz). This limits the rise-time to $\tilde{}$ 3 nsec, whereas our time domain reflectometer has 0.17 ns rise-time or 2000 MHz equivalent bandwidth. Even if we would have the costly data acquisition systems or network analyzers, needed to measure further, one could hardly imagine how complicate a plot of $Z(\omega)$ would look like if all the spirals would be measured over a 20 times longer frequency range. Even if the person who will measure in the future would have time for measurements over wide frequency ranges, it is even less probable that a member of the machine study team would have time to transform the measured data by means of Smith charts or computers to find out their correct value. If not the effort on data acquisition would be useless.

Since the direct Laplace transform is easier to be done analytically than its inverse, all general theorems on Laplace transforms (or equivalent ones on Fourier-, Mellin-, or Z-transforms) and tables[8] can be used in theoretical studies to obtain even analytical expressions of $\rho(\omega)$ from measured traces of $\rho(t)$. Such expressions are easier to handle than large amounts of data for every straight section. The inverse formula of equ. (21) is

$$\rho(j\omega) = j\omega.L(\rho(t)) = s.L(\rho(t)) \qquad (22)$$

Transmission coefficients can also be measured in the time domain. Consequently a complete characterization of a two-port in the time domain is possible in principle.

11. Some pratical aspects of time domain reflectometry.

Available TDR's have usually 50 Ω source impedance. The transition from 50 Ω to 125 Ω should not be accomplished by a minimum loss L-pad which matches both incident and reflected wave because it also attenuates incident and reflected voltage and for our high impedance ratio 2.5 the reflected signal becomes noisy. Moreover it is not easy to make a precise L-pad for 2000 MHz. It is easier and better to match only the reflected voltage (to avoid multiple reflections) by means of a 75 Ω series resistor between the 125 Ω and 50 Ω system. This leaves the incident voltage $V_o/2 = 1$ and divides the returning voltage into 50/125 = 40% because the series resistor cannot alter the reflected current. Therefore the vertical deflection of the oscilloscope must be increased by the factor 2.5 and recalibrated for $\rho = \pm 1$ by means of an open and short circuit at the end of the 125 Ω line. A similar 75 Ω series resistor in front of a matched 50 Ω (or 50 Ω + matched 75 Ω cable) is used to terminate the line and allow to measure the transmitted signals in a standard 50 Ω system. When a centre conductor of 2 mm diameter with $Z_o = 228$ Ω is used (to test for instance RF-cavities) matching with a 178 Ω series resistor is done inside the vacuum chamber. The 125 Ω system permits the use of precise connectors type "Berkeley 125 Ω " from stores and N or C-connectors for 50Ω but in no case BNC! Even with good connectors there are mismatches at the soldered feedthrough into the tank. It is practically impossible to correct these errors in the frequency domain because the small reflection affects the whole spectrum whereas in the time domain it is localized and can therefore be shifted out of the display or be deliberately ignored in interpretations.

Reflectometry in time or frequency domain allows to measure resistances in the range $-0.9 < \rho < +0.9$ or the resistance range 6 Ω < R < 2400 Ω with $Z_o = 125$ Ω and small differences $Z_o + \Delta Z$ with ΔZ a few ohms per straight section. This is adequate because the sum of impedances for 100 straight sections should be well below the kiloohm range and if one straight section shows higher impedances something has to be done anyway. The shunt resistances of resonant cavities fall into this category and are measured by other methods too. It is however good to measure them with TDR in order to have an impartial basis for comparison with all other kind of hardware even if the absolute ohm values are not known exactly.

12. Interpretation of the reflection coefficient $\rho(t)$.

A) Lumped component circuits : In a similar way as one can recognize in a Smith chart plot the presence of a capacitor C or inductor L connected in series or in parallel with a constant resistance R = 1/G and determine the component values one can also recognize each of these 4 equivalent circuits from a display of the reflection coefficient in the time domain and determine R and L or C.

In all four cases $\rho(t)$ is an exponential function which rises for (charging) capacitors and falls for inductors. The necessary formulas can be derived from our equivalent test circuit which shows the generator with source impedance Z_o connected in series with the input impedance of the circuit under test. For an inductor the reflected voltage is

$$\rho(t) = V(t) - 1 = 2\, e^{\frac{-Z_0 t}{L}} - 1 \qquad (23)$$

and for a capacitor

$$\rho(t) = (2 - 2\, e^{-\frac{t}{Z_0 C}}) - 1 = -2\, e^{-\frac{t}{Z_0 C}} + 1 \qquad (24)$$

The exponential time constant $\tau = L/Z_o$ or $Z_o C$ can be determined on the photographed signal. It yields the value of L or C

$$L = \tau \,.\, 125\,\Omega \qquad \text{or} \qquad C \,.\, \tau/125\,\Omega \qquad (25)$$

It has already been mentioned that if the time domain reflectometer display has an ohm-scale overlay to convert ρ into resistance values, one can read the dc-resistance $Z(\omega)$ for $\omega \to 0$ from the asymptotic value $\rho(t)$ for $t \to \infty$. Similarly the high frequency resistance $Z(\omega)$ for $\omega \to \infty$ (where capacitors are considered as short circuits and inductors as open circuits) is the value $\rho(t)$ at the start $t \to 0$ with $t > 0$. These limiting cases indicate whether a series or shunt resistor is present. If $\rho(t)$ falls or rises between the limits ρ_{min} and + 1, the value ρ_{min} indicates the value of a series resistor. Since this series resistor adds to $Z_o = 125\ \Omega$ one has in this case

$$L = \tau(125\,\Omega + R_s) \quad \text{or} \quad C = \tau/(125\,\Omega + R_s) \tag{25a}$$

If however ρ varies between -1 and ρ_{max} the reactance is shunted by a parallel resistor R_p and ρ_{max} indicates its value on the ohmscale. In this case the element values are

$$L = \tau/(\frac{1}{125\,\Omega} + \frac{1}{R_p}) \quad \text{or} \quad C = \tau(\frac{1}{125\,\Omega} + \frac{1}{R_p}) \tag{25b}$$

This can be seen when the voltage generator with 125 Ω series resistance is replaced (by Thevenins theorem) by a current generator with 125 Ω resistance connected in parallel.

B) Interpretation of small wall impedances : In our measurements the series resistance is often given by the value $Z_o = 125\ \Omega$ of a matched PS-vacuum chamber. If a lumped, complex wall impedance $\Delta Z(s) = \Delta Z(j\omega)$ is encountered the input impedance

$$Z = \Delta Z + Z_o \tag{26}$$

yields the reflection coefficient (equ.(8))

$$\rho(s) = \frac{(Z_o + \Delta Z) - Z_o}{(Z_o + \Delta Z) + Z_o} = \frac{\Delta Z}{2Z_o + \Delta Z} \tag{27}$$

If $\Delta Z << 250\ \Omega$ - hopefully in most straight sections - one obtains simply

$$\Delta Z(s) \approx \rho(s)\ .\ 250\ \Omega = 250\ \Omega.s.L(\rho(t)) \tag{28}$$

C) Resonances : The most frequently observed signal (e.g. Fig. 6) is a damped oscillation

$$\rho(t) = \rho_o e^{-\sigma t} \sin \omega_1 t \tag{29}$$

which is characterized by the constants ρ_o, σ, ω_1. Its Laplace transform

$$L(\rho(t)) = \frac{\rho_0 \omega_1}{(s+\sigma)^2 + \omega_1^2} \tag{30}$$

is substituted in equation (28) to obtain ρ in the frequency domain

$$\rho(s) = sL(\rho(t)) = \frac{s\rho_0 \omega_1}{s^2 + 2\sigma s + (\omega_1^2 + \sigma^2)} \tag{31}$$

We return to equation (22) which can be written in terms of admittances (assuming $2Z_o = 250\ \Omega$)

$$\rho_s = \frac{1/250\ \Omega}{1/\Delta Z + 1/250\ \Omega} \tag{27a}$$

and substitute for $1/\Delta Z$ the admittance of an equivalent parallel resonant circuit

$$\frac{1}{\Delta Z} = sC + \frac{1}{sL} + \frac{1}{R} \tag{32}$$

$$\rho(s) = \frac{1/250\ \Omega}{sC + \frac{1}{sL} + (\frac{1}{R} + \frac{1}{250\ \Omega})} = \frac{s/(C.250\ \Omega)}{s^2 + \frac{s}{C}(\frac{1}{R} + \frac{1}{250\ \Omega}) + \frac{1}{LC}} \tag{33}$$

Comparison of the coefficients in equations (33) and (31) yields all 3 component values :

$$\boxed{\begin{aligned} C &= \frac{1}{250\ \Omega\ \rho_0 \omega_1} \\ L &= \frac{1}{C(\omega_1^2 + \sigma^2)} \\ R &= \frac{1}{2\sigma C - 1/250\ \Omega} = \frac{250\ \Omega}{\frac{2\sigma}{\rho_0 \omega_1} - 1} \end{aligned}} \qquad (34) - (37)$$

1/R is the shunt conductance of the equivalent circuit and

$$\frac{1}{R'} = \left(\frac{1}{R} + \frac{1}{250\ \Omega}\right) = 2\sigma C \tag{38}$$

is the shunt conductance of the loaded equivalent circuit. The expression (37) for the shunt impedance R becomes inaccurate if R > 200 Ω because the difference between 2σC and 1/250 Ω in the denominator becomes small. In such cases one can use a thinner center conductor of higher Z_0. The time domain reflectometer is a good method for recording the majority of smaller coupling impedances but in the case of very high shunt impedances of resonant cavities additional measurements with a vector impedance meter or at high frequencies with perturbation methods*) are required. Better decrease or eliminate them from the PS -. For a parallel resonant circuit R can also be expressed as the product of the characteristic impedance $\sqrt{L/C}$ and the Q-value

$$R = Q.\sqrt{L/C} \tag{39}$$

It is interesting for the interpretation that $\sqrt{L/C}$ is just the observed oscillation amplitude ρ_0 times 250 Ω

$$\underline{\rho_0 . 250\ \Omega = \frac{1}{\omega_1 C} \approx \sqrt{\frac{L}{C}}} \tag{40}$$

where $$\omega_1 = \sqrt{\omega_0^2 - \sigma^2} \approx \omega_0 = \frac{1}{\sqrt{LC}} \tag{41}$$

These formulas for equivalent circuits should simplify the necessary quantitative comparisons between different equipment in various straight sections because in a vacuum tank which contains high voltage plates or septum magnets the impedance ΔZ(s) cannot directly be measured as easily as on the gap of an accelerating cavity. Sometimes ΔZ(s) represents the transformed impedance of some loosely coupled oscillating circuit as seen from the position of the centre conductor (or beam). Equation (29) implies the initial condition ρ(t) = 0 at t = 0, which is plausible when the transit time through the tank is short and ρ(t) ≈ 0 after this time because the tank is terminated in 125 Ω. The oscillation is often superposed to some other

*) G. Dôme in CERN LAB 2 measured the shunt resistance R of the 200 MHz cavity by the perturbation method.

signal which can be interpreted separately to simplify the problem. Often two or more modes of different frequencies are important in a resonant cavity and are excited at the same time by the step pulse. Then one can determine an equivalent circuit for each mode. However, qualitatively one can say that the modes with largest amplitude and longest damping time constant $1/\sigma$ contribute most to $|Z|/n$, as defined in the coasting beam stability criterion [1,2]. This rule of thumb becomes plausible if one divides expression (39) by the harmonic number n at resonance frequency

$$n = \frac{f_1}{f_{rev}} = \frac{\omega_1}{\omega_{rev}} \tag{42}$$

$$\frac{|Z|}{n} = \frac{R}{\omega_1/\omega_{rev}} = \omega_{rev} \left(\frac{Q}{\omega_1}\right)\sqrt{\frac{L}{C}} \tag{43}$$

$\sqrt{L/C}$ increases with the amplitude ρ_0 and Q/ω_1 increases with the exponential damping time constant $1/\sigma$ (as long as the resonant circuit is not too much damped by the termination resistors $2 \times Z_o = 250\ \Omega$).

D) Equivalent circuit for septum tank S.S.74.

$$f_1 = 1/14.5 \text{ ns} = 69 \text{ MHz} = \omega_1/2\pi$$

$$\sigma = 1/100 \text{ ns} = 10 \text{ MHz}$$

$$\rho_0 = 0.02$$

one obtains

$$C = 0.46 \text{ nF}$$

$$L = 11.5 \text{ nH}$$

$$\underline{R = 191 \ \Omega}$$

$$\sqrt{L/C} = 5 \ \Omega$$

$$Q = 191/5 = 38.2$$

Finally

$$\frac{|Z|}{f_1} = \frac{191 \ \Omega}{69 \text{ MHz}} = 2.77 \ \Omega/\text{MHz}$$

$$\underline{\frac{|Z|}{n}} = \frac{|Z|}{f_1} \cdot f_{rev} = \underline{1.32 \ \Omega}$$

The values of R and $|Z|/n$ are estimated to be known to 20% accuracy.

E) <u>Distributed circuits</u>. At very high frequencies i.e. when observing small details of the display $\rho(t)$ at fast sweep rates of 1-4 nsec/div or 15-60 cm/div displayed electrical length, the distributed capacity per length C' between the centre conductor and wall becomes as important as the distributed inductance per length L'. The square root of their ratio

$$\sqrt{L'/C'} = Z'_o = 60 \, \ln \frac{b}{a} \tag{47}$$

and their product

$$\sqrt{L'.C'} = \frac{1}{\beta \bar{c}} \approx \frac{1}{\bar{c}} \tag{48}$$

are more suitable quantities to be observed versus travel-around-time than L' and C' themselves, because essentially only the ratio Z'_o varies. Equation (47) which gives the characteristic impedance Z'_o for a vacuum tank of circular cross section can be used to determine the outer radius b

$$b = a \, \ln^{Z'_o/60\,\Omega} \tag{49}$$

This is useful for all those tanks which have a very complicated cross section or are filled with hardware which makes it almost impossible to calculate the beam potential. In this case an exact measurement of

$$Z'_o = 125\ \Omega + \Delta Z \tag{50}$$

with respect to a 125 Ω reference allows to determine the equivalent radius b in equ. (49) and to calculate the beam potential everywhere in the PS. The beam potential must be known for the negative mass instability and resistive wall instability. For the standard elliptic vacuum chamber one has the equivalent radius

$$b_o = 4.316 \text{ cm}$$

The next measurable quantity is 2 τ. τ is the time required to traverse the electrical length of the non-standard vacuum chamber. (transit time). Results for septum magnet tank S.S.74, Fig. 7 :

$\rho = 0.18$, $Z_o' = 180\ \Omega$, $b = 10$ cm.

$2\tau \approx 7$ ns

The values of ρ and τ agree sufficiently with the results obtained in the frequency domain but are more reliable because the photos show more detail of the "square pulse" 0.18 x 7 nsec.

F) Multiple reflections. A length of non-standard vacuum chamber inserted between infinite (or matched) standard vacuum chambers forms a damped resonant transmission lines because the discontunuities at both ends reflect waves. The reflected waves cannot escape the section immediately and the ratio of energy stored per cycle per energy lost per cycle can be regarded as the Q-value of a resonant transmission line section or cavity with centre conductor. Such a vacuum chamber section of larger radius b may also disturb the beam if b is big and even more if this is the case for many straight sections at regular intervals[12]. The data b and τ can be used as a basis for theoretical studies on the PS.

However such multiple reflections between a pair of discontinuities may not only disturb the beam but also the accuracy of time domain reflectometry because for large radii b multiple reflections are observed on the display :
Assume the unit step encounters the first discontinuity and ρ is reflected while $1-\rho$ is transmitted. After the delay τ the latter encounters $-\rho$ because seen from the inside Z_o' and Z_o exchange their rôles in equ. (8). $-\rho(1-\rho)$ is reflected. It travels back and after 2τ it encounters the first discontinuity with $-\rho$ and

$$-\rho(1-\rho)(1+\rho) = -\rho(1-\rho^2) = -\rho + \rho^3 \qquad (51)$$

is reflected back to the oscilloscope. Therefore $\rho(t)$ does not return exactly to zero level as it should for $Z_o = 125\ \Omega$ but only to ρ^{+3} because of multiple reflections. The reflectometer doesn't indicate the correct impedance level for the second and later reflections, because each discontinuity reflects some power and takes it from the unit step pulse which becomes smaller and smaller. However due to the choice of a high $Z_o = 125\ \Omega$ ρ is often small

$$\rho \approx \frac{\Delta Z}{250\ \Omega} < 0.1 \qquad (52)$$

and the terms of the order ρ^3 negligible. Only for very large discontinuities one observes further reflections because the returning pulse $-\rho(1-\rho)$ is reflected at the first discontinuity $-\rho$ and travels again in forward direction with the amplitude $\rho^2(1-\rho)$ i.e. ρ^2 times less. Therefore after the first "square pulse" of hight ρ one observes after periods 4τ an infinite series of further square pulses with exponentially decreasing amplitudes $(\rho^2)^n$.

G) Resistive walls : Neglecting multiple reflections for $\rho < 0.1$, one can assume that TDR gives a display of real impedances $Z = R(t)$ or $R(x)$ if the time base is recalibrated in units of electrical length x (o.15 m/nsec). Then a distributed resistive wall impedance is observed as a positive slope

$$R' = \frac{dR}{dx} \approx \frac{d\rho}{dx} \cdot 250\ \Omega \qquad (53)$$

Resistive walls are of course important for the assessment of the resistive wall instability in the PS. If for instance a standard chamber has a total wall impedance of 25 Ω , $\rho(t)$ would be a positive slope indicating the maximum value 125 Ω + 25 Ω and 25 Ω would be the integral $\int R'dx$. On the other hand a positive slope could also mean that the radius and characteristic impedance Z_o of a vacuum chamber increase.

However at the end where it is connected to the standard 125 Ω-vacuum chamber $\rho(t)$ would drop back to zero whereas in the case of a resistive wall it remains on the high level 125 Ω + ΔR. Thus one can distinguish the two cases.

A distinction is also possible by comparison of the transmission coefficients s_{12}. In a lossless vacuum tank the s-parameters are related because the transmitted power is just the incident power minus reflected power. At every frequency one has

$$|s_{12}|^2 = 1- |s_{11}|^2$$

whereas in presence of resistive walls $|s_{12}|$ is smaller. The time domain reflectometer does not show the very small wall resistance of few milli-ohm of a stainless steel chamber but rather the more important contributions of several ohms of metal coated ceramic vacuum chambers which are needed for fast magnets. The resistance of the center conductor itself should also be subtracted but it is usually negligible.

It would lead too far to continue the discussion of pulse response of circuits and time domain reflectometry [13,14]. We shall not interpret oscillations between 1-2GHz which are visible but would lead to the more specialized subject of pulse transmission in waveguides and cannot be discussed without a large background on waveguide mode propagation.

Only the most typical encountered reflections $\rho(t)$ have been interpreted with the aim of finding the simplest equivalent circuits and excluding those equivalent circuits which are not probable in our context.

13. Final remark.

TDR gives an idea of the voltage transients which will be excited by the beam and act on it. Although the test pulse is a normalized unit step one can either differentiate this signal and obtain the response to a short impulse similar to a short bunch or even use convolution computer programs to calculate the transient voltage for any desired bunch shape. Both TDR signals and pick-up signals of the bunch shapes are in the time domain. Therefore common oscillation periods can be recognized by direct comparison of photos. (Comparison in the frequency domain requires a Spectrum analyzer for the pick-up signal and a network analyzer for the reflected test signal). Few photos of $\rho(t)$ obtained with several sweep speeds contain all information about the impedance of the beam environment in a very condensed and directly interpretable form.

14. Acknowledgements.

I thank E. Brouzet, J. Gareyte and D. Möhl for reading this manuscript and for their comments.

REFERENCES

1. E. KEIL and W. SCHNELL : "Concerning Longitudinal Stability in the ISR" CERN - ISR - TH - RF/69-48

2. A.M. SESSLER - 1971 Particle Accel. Conf. IEEE - Transactions on Nucl. Science Vol. 18, page 1039.

3. H.H. UMSTÄTTER : Evaluation of the Stability Criterion for a Coasting Beam in the PS. (a coupling impedance diagram). MPS/SR/note 73-29.

4. H.H. UMSTÄTTER : On the transmission of signals by the wide band pick-up station. MPS/Int. SR 68-2.

5. K. KUROKAWA : Power Waves and the Scattering Matrix. IEEE Transactions on Microwave Theory and Techniques Vol MTT-13 p. 194-202 (1968)

6. "S-Parameters... Circuit Analysis and Design. A Collection of articles". Hewlett Packard Application Note 95 (sept 1968).

7. L. HUELSMAN : Circuits, matrices and linear vector spaces. Mac Graw Hill (N.Y. 1963). Section 3.7 The Scattering matrix.

8. R.V. CHURCHILL : Modern Operational Mathematics in Engineering. Mc Graw Hill Book Comp. (New York 1944).

9. H.H. UMSTÄTTER : Coupling Impedance test on the IBS for the PS and booster. MPS/SR/Note 72-32.

10. D. MÖHL and H.H. UMSTÄTTER : Estimates of the transverse coupling impedance of the inflector system (s.s.26). MPS/DL/Note 73-6.

11. H.H. UMSTÄTTER : Coupling impedance measurements on the FAK with the TDR. MPS/SR/Note 73-25.

12. E. KEIL and B. ZOTTER : Longitudinal stability of a coasting beam in a corrugated resistive vacuum chamber. Particle Accelerator. Vol 3, p.11. (1972)

13. Time domain reflectometry. Hewlett Packard Application Note 62.

14. A.A. STRICKLAND, H.A. ZIMMERMAN, G. LONG and G.FRYE : Time domain reflectometry measurements. 107 p. Tektronix Inc. (1970).

Table 1. Impedance $Z(\omega)$

f[MHz]	|Z|	arc(Z)	f[MHz]	|Z|	arc(Z)
0.5	126.	1.	1.0	129.	1.
3.	127.	3.	5.	129.	6.
7.	134.	8.	10.	137.	10.
15.	147.	13.	20.	156.	15.
25.	166.	17.	35.	201.	16.
40.	220.	13.	52.	238.	-1.
56.	229.	-6.	60.	194.	-7.
61.8	166.	-1.	63.	156.	16.
64.5	291.	33.	66.	378.	5.
67.	345.	-7.	68.	315.	-12.
70.	288.	-18.	80.	214.	-26.
90.	188.	-29.	100.	165.	-27.

Table 2. Reflection coefficient $\rho(\omega)$

f[MHz]	|ρ|	arc(ρ)	f[MHz]	|ρ|	arc(ρ)
.5000	.0096	65.4600	1.0000	.0180	28.9854
3.0000	.0274	73.1269	5.0000	.0547	73.2277
7.0000	.0781	63.4364	10.0000	.0988	62.1377
15.0000	.1397	54.1012	20.0000	.1717	49.2060
25.0000	.2053	45.4820	35.0000	.2721	29.2069
40.0000	.2979	20.6811	52.0000	.3114	-1.4502
56.0000	.2984	-9.2324	60.0000	.2248	-15.0312
61.8000	.1412	-3.4739	63.0000	.1786	50.9809
64.5000	.4935	29.8461	66.0000	.5048	3.7030
67.0000	.4719	-5.8045	68.0000	.4440	-11.0811
70.0000	.4244	-18.2889	80.0000	.3490	-37.8590
90.0000	.3273	-49.1272	100.0000	.2767	-58.2250

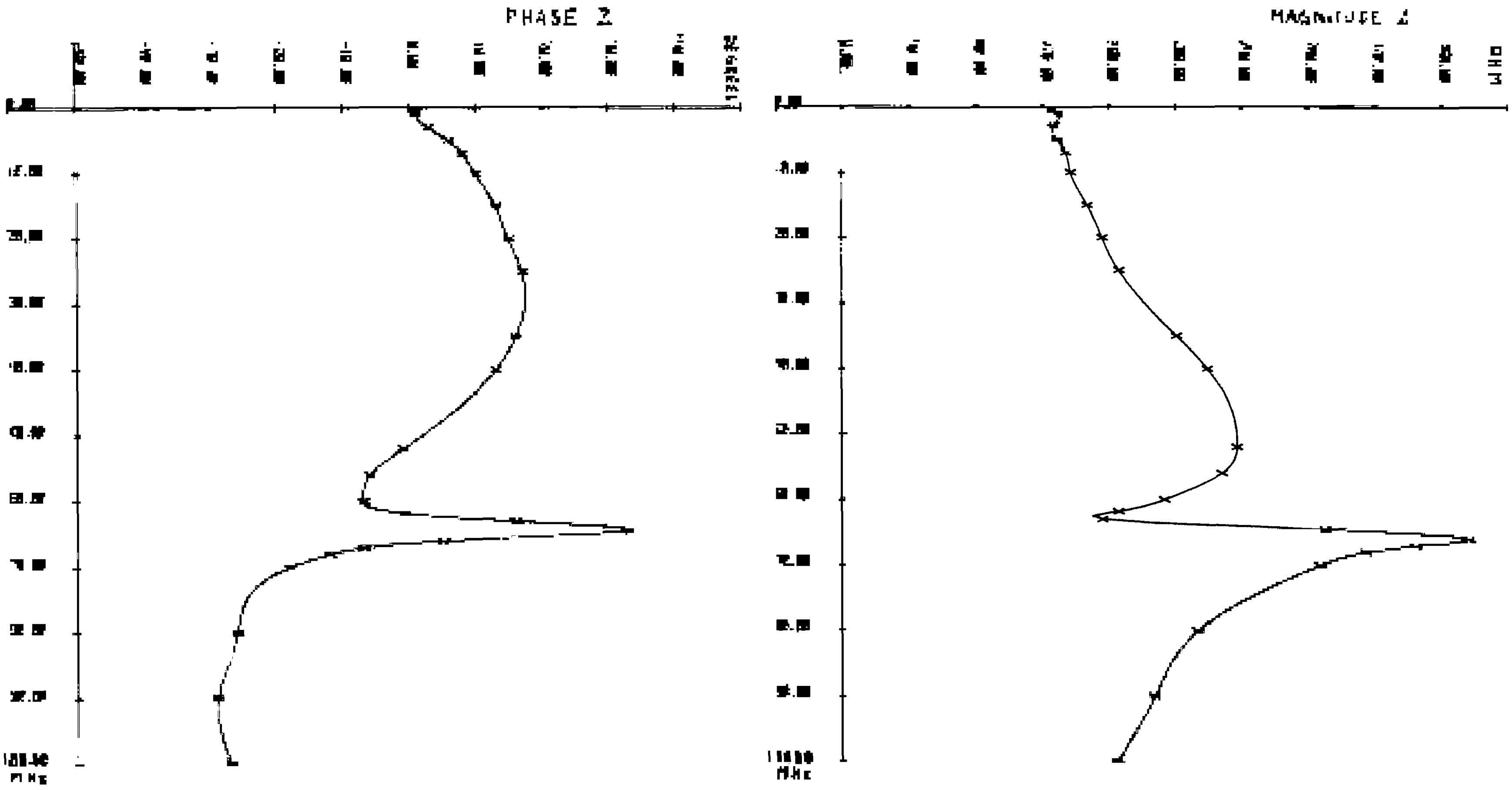

FIG. 1: Impedance versus frequency

FIG. 2: Reflection coeff.

Magnitude & Phase
0 - 100 MHz
(centre = z_o = 125 Ω)

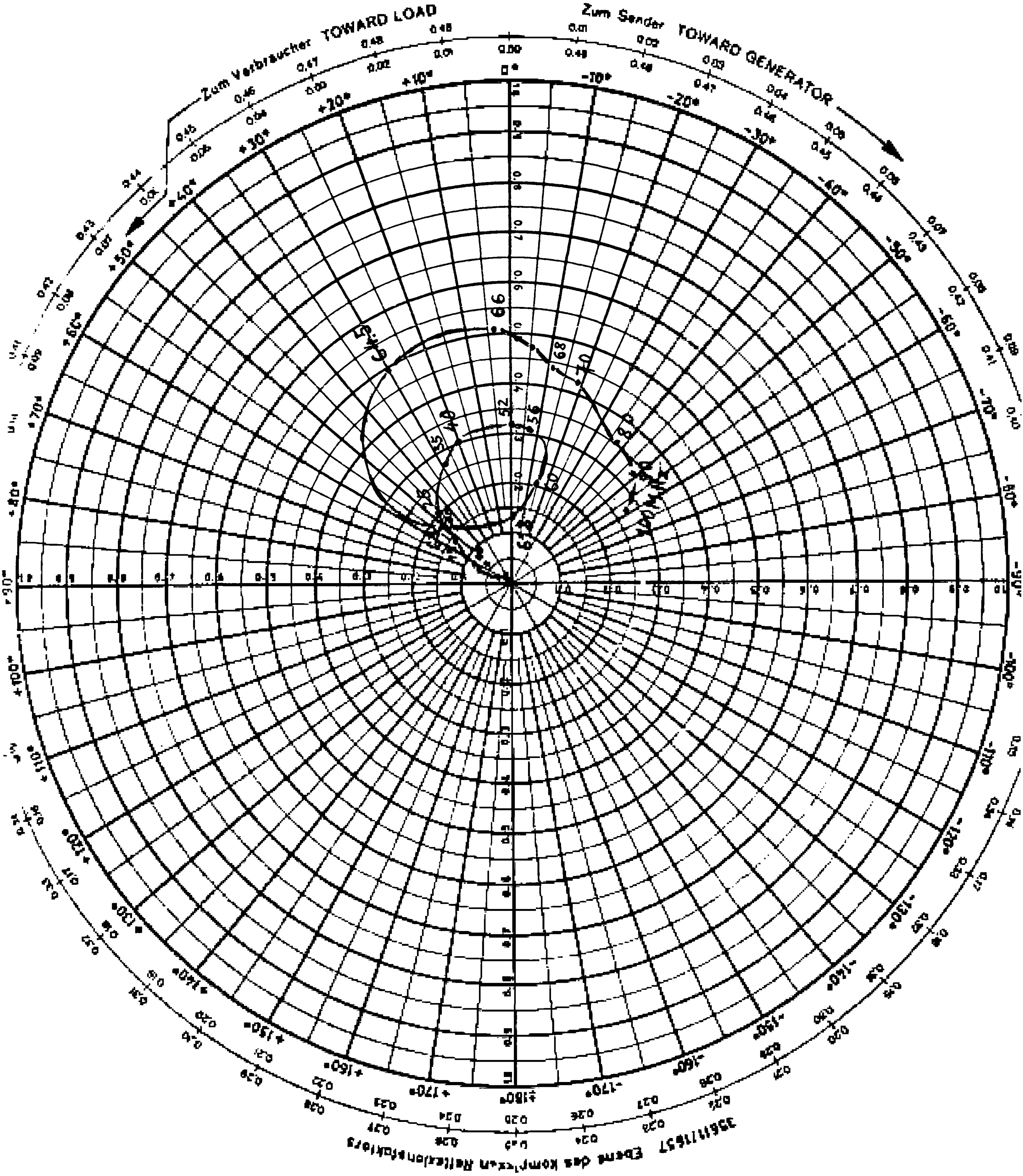

FIG. 3: Impedance
resistance and reactance
"Smith Chart" 125 Ω = 1

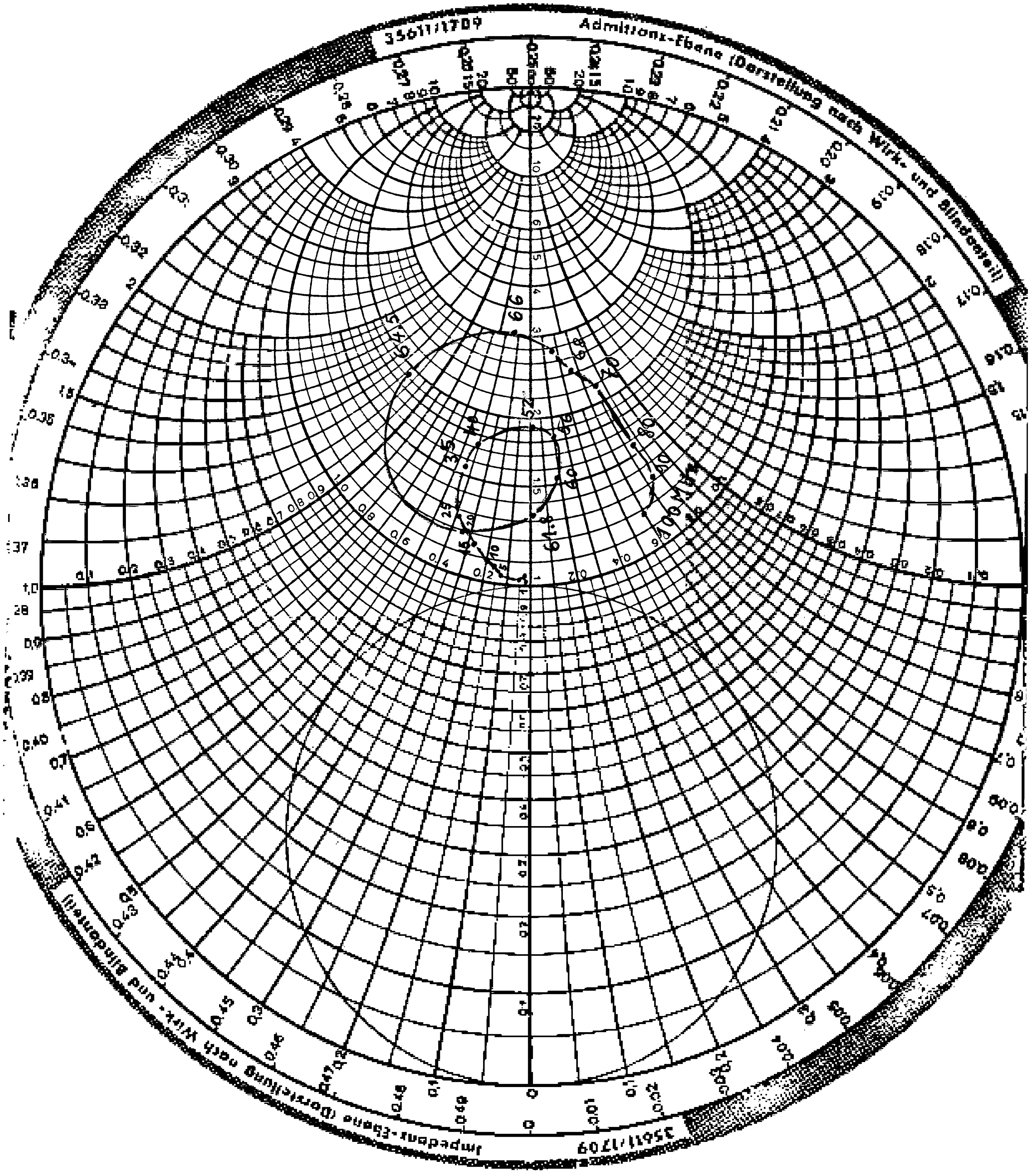

FIG. 4: Impedance

magnitude and phase

"Carter Diagram" 125 Ω = 1

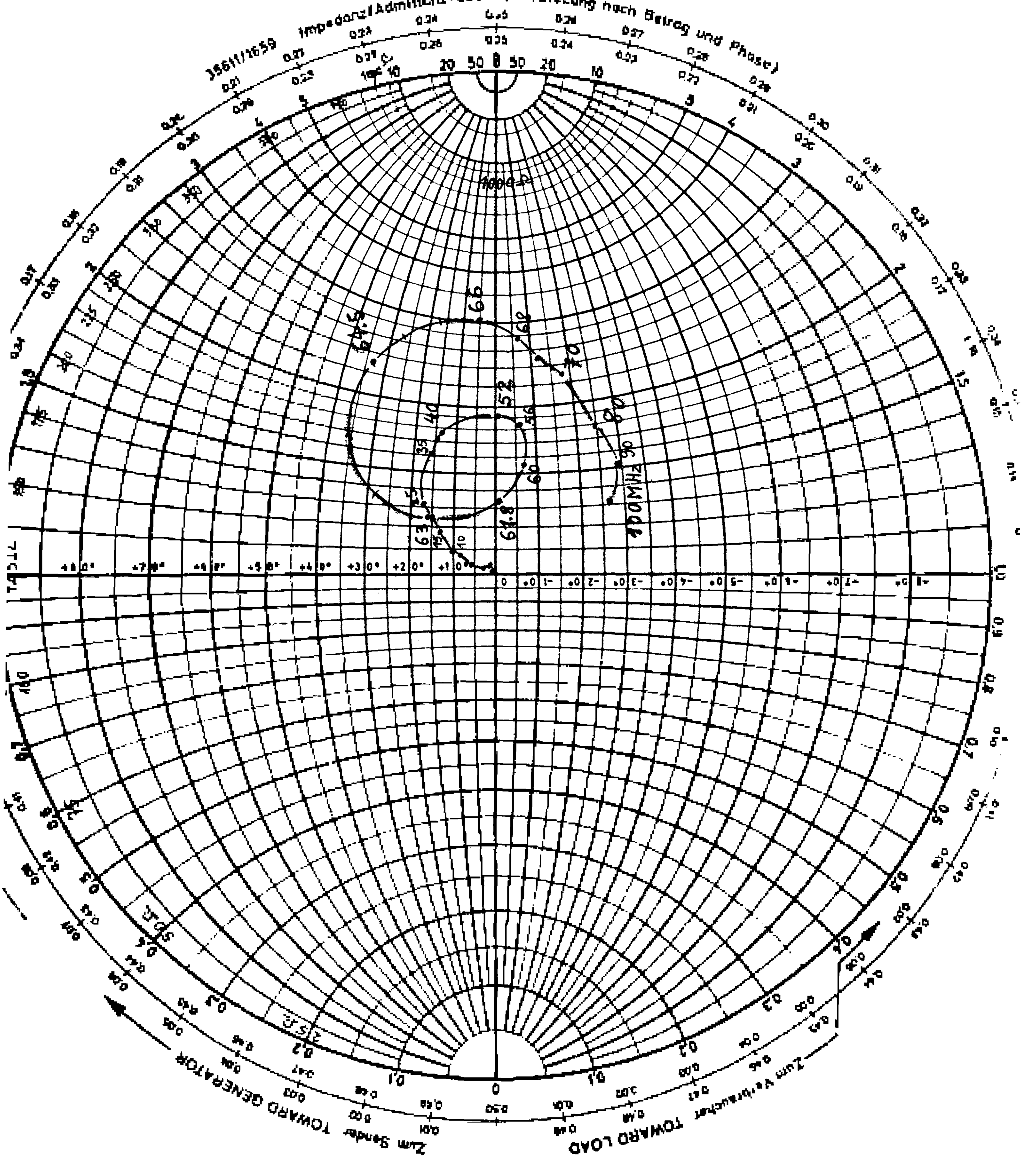

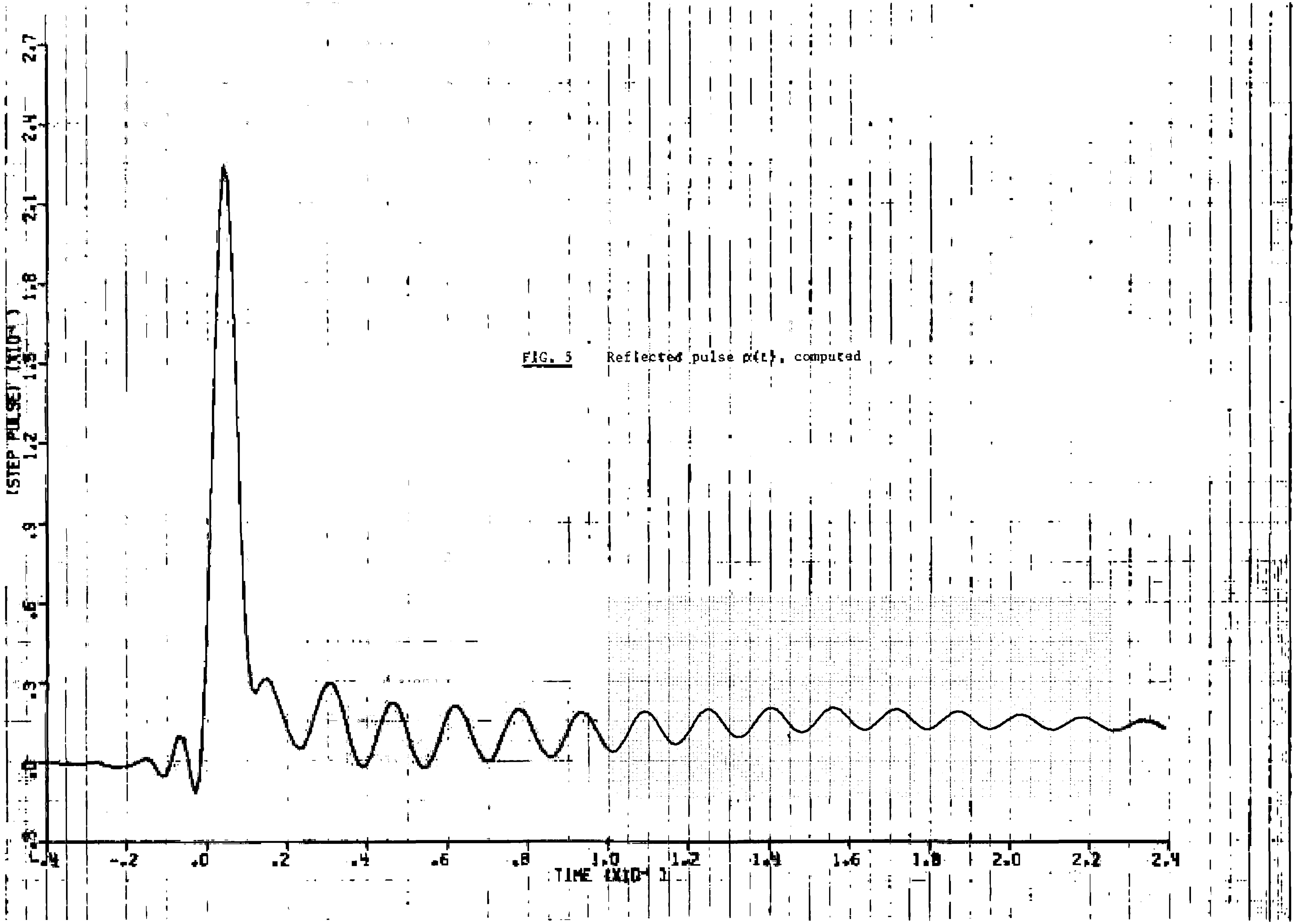

FIG. 5 Reflected pulse $p(t)$, computed

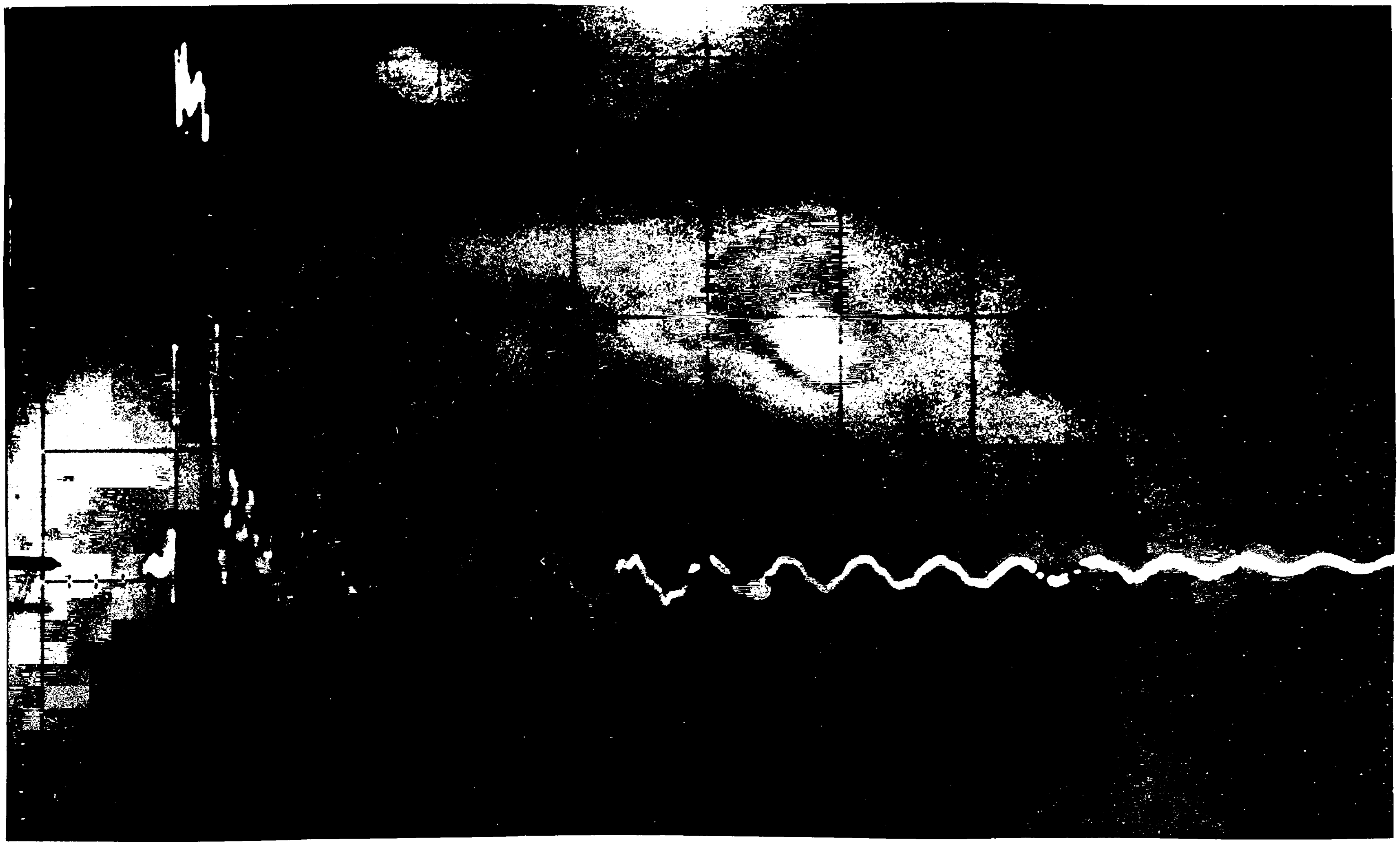

Fig. 6

Reflected pulse
vertical scale ρ = 0.05/div 25 nsec/div

Reflection coefficient in the time domain

vertical scale: ρ=0,05/div

FIG. 7

4 nsec/cm

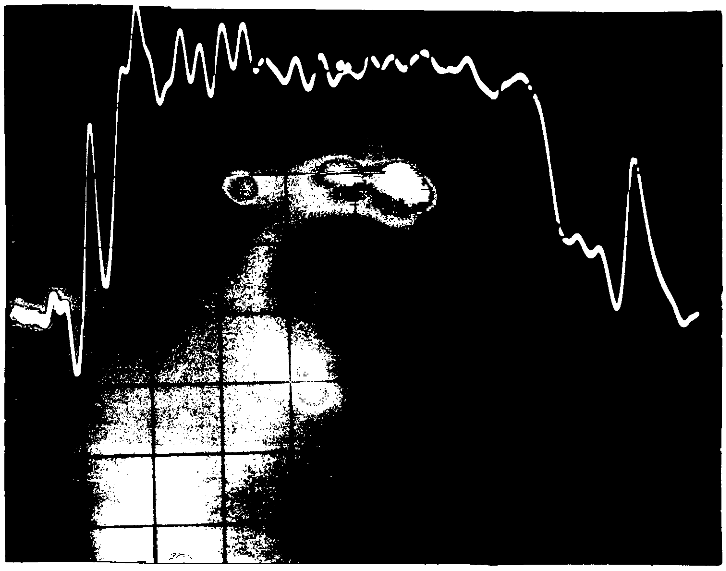

FIG. 8

1 nsec/cm

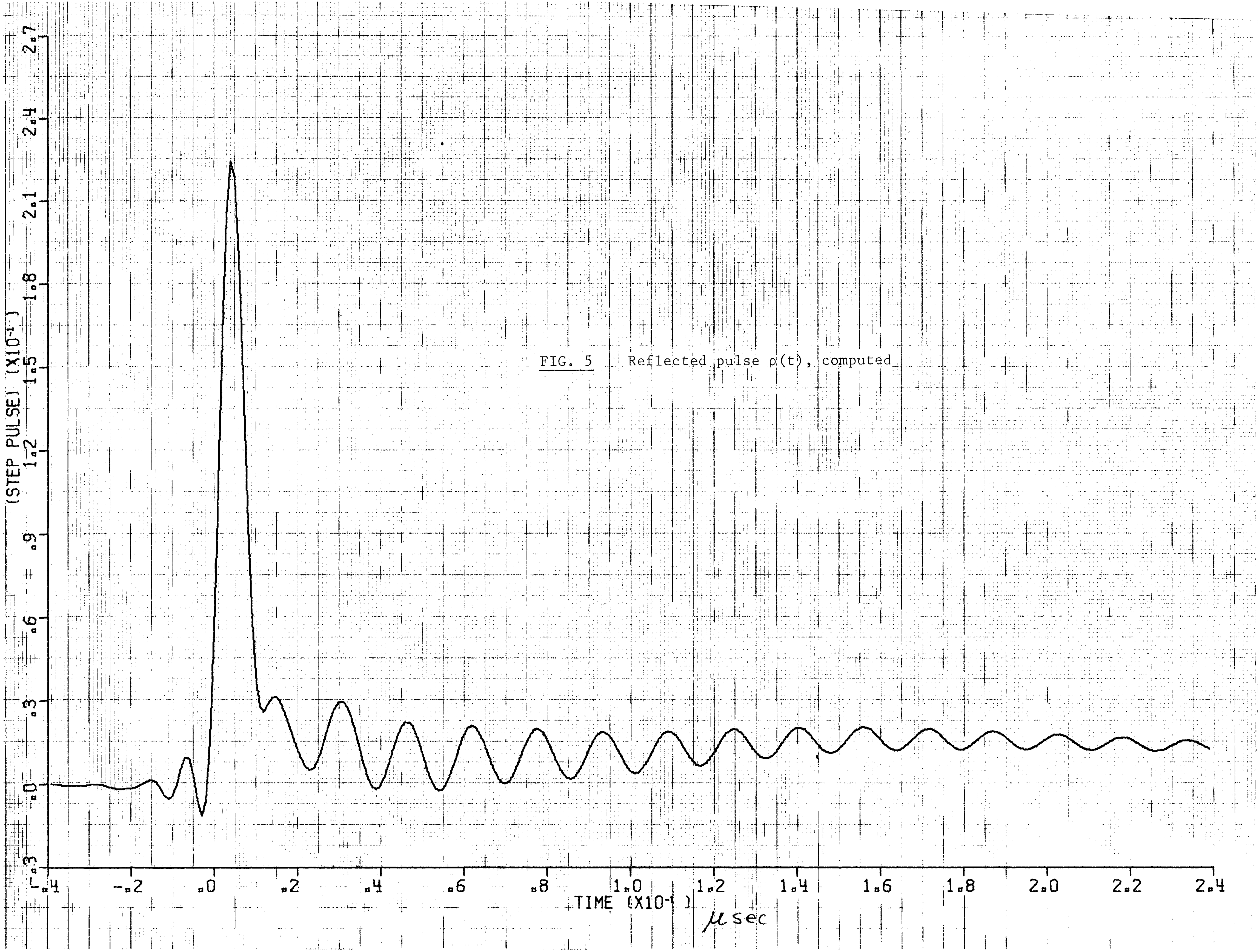

FIG. 5 Reflected pulse ρ(t), computed